Technical Report ARAED-TR-96020

CONSTANT CRITICAL STRAIN FOR MECHANICAL FAILURE OF SEVERAL PARTICULATE POLYMER COMPOSITE EXPLOSIVES AND PROPELLANTS AND OTHER EXPLOSIVES

Donald A. Wiegand

July 1997

U.S. ARMY ARMAMENT RESEARCH, DEVELOPMENT AND ENGINEERING CENTER

Armament Engineering Directorate

Picatinny Arsenal, New Jersey

US ARMY
TANK AUTOMOTIVE AND
ARMAMENTS COMMAND
ARMAMENT RDE CENTER

REPORT DOCUMENT PAGE

Form Approved
OMB No. 0704-0188

Public reporting burden for this collection of information is estimated to average 1 hour per response, including the time for reviewing instruction, searching existing data sources, gathering and maintaining the data needed, and completing and reviewing the collection of information. Send comments regarding this burden estimate or any other aspect of this collection of information, including suggestions for reducing this burden, to Washington Headquarters Services, Directorate for Information Operations and Reports, 12115 Jefferson Davis Highway, Suite 1204, Arlington, VA 22202-4302, and to the Office of Management and Budget, Paperwork Reduction Project (0704-0188), Washington, DC 20503.

1. AGENCY USE ONLY (Leave blank)	2. REPORT DATE July 1997	3. REPORT TYPE AND DATES COVERED

4. TITLE AND SUBTITLE
CONSTANT CRITICAL STRAIN FOR MECHANICAL FAILURE OF SEVERAL PARTICULATE POLYMER COMPOSITE EXPLOSIVES AND PROPELLANTS AND OTHER EXPLOSIVES

5. FUNDING NUMBERS

6. AUTHORS
Donald A. Wiegand

7. PERFORMING ORGANIZATION NAME(S) AND ADDRESS(ES)

ARDEC, AED
Energetics Warheads Division (AMSTA-AR-WEE-D)
Picatinny Arsenal, NJ 07806-5000

8. PERFORMING ORGANIZATION REPORT NUMBER

9. SPONSORING/MONITORING AGENCY NAME(S) AND ADDRESS(ES)

ARDEC, LSED
Information Research Center (AMSTA-AR-LSL)
Picatinny Arsenal, NJ 07806-5000

10. SPONSORING/MONITORING AGENCY REPORT NUMBER

Technical Report
ARAED-TR-96020

11. SUPPLEMENTARY NOTES

12a. DISTRIBUTION/AVAILABILITY STATEMENT

Approved for public release; distribution is unlimited.

12b. DISTRIBUTION CODE

13. ABSTRACT (Maximum 200 words)
The mechanical response in compression of several polymer composite explosives and propellants and two other explosives was determined as a function of temperature and strain rate. The compressive strength (maximum stress) and the apparent modulus increase with decreasing temperature and increasing strain rate, are proportional to each other. While the compressive strength and the modulus vary by about an order of magnitude, the strain at the maximum stress is approximately constant with variations of strain rate and temperature. This approximately constant strain can be used as a criterion for failure, and suggests a critical local strain or displacement for failure.

14. SUBJECT TERMS

Polymer composite	Critical strain	Compressive strength	Yield
Interface failure	Fracture	Plastic flow	Modulus

15. NUMBER OF PAGES 18

16. PRICE CODE

17. SECURITY CLASSIFICATION OF REPORT UNCLASSIFIED	18. SECURITY CLASSIFICATION OF THIS PAGE UNCLASSIFIED	19. SECURITY CLASSIFICATION OF ABSTRACT UNCLASSIFIED	20. LIMITATION OF ABSTRACT SAR

NSN 7540-01-280-5500

Standard Form 298 (Rev. 2-89)
Prescribed by ANSI Std Z39.18
298-02

ACKNOWLEDGMENTS

CONTENTS

INTRODUCTION

This work was initiated to survey the mechanical properties of a group of particulate polymer composite explosives (refs 1 and 2) and is expanded here to include composite propellants and other explosives (ref 3). The polymer composites are made up of polymer binders (with plastizer in most cases) and 48% to 95% organic polycrystalline non-polymer explosive fillers (table 1). One non-polymer composite, Composition B, and the binder for this composite, TNT, are also considered. The general approach of the work presented was to determine the stress versus strain properties of these composites as a function of temperature and strain rate over the military ranges of interest. The condition of the samples after deformation was also noted, i.e., whether there was evidence of plastic deformation, cracking, and/or fracture.

EXPERIMENTAL

Stress versus strain data in compression were obtained using an MTS servo-hydraulic system operated at constant strain rates of 0.001 to 30/s (ref 4). Samples were in the form of right circular cylinders 1/4 in. to 1 in. in length and 1/4 in. to 3/4 in. in diameter and the end faces of the samples were coated with a lubricant (e.g., graphite) to minimize frictional effects between the sample and the loading platens. Samples were conditioned at temperatures between -60° and 75°C for at least 2 hrs before measurements. Samples were compressed along the cylinder axis and engineering stress and strain obtained. One to five samples were measured at each temperature and strain rate.

Samples of the polymer composite explosives were prepared either by pressing to size or by pressing into large billets and machining to size (refs 1, 2, and 5). The composite propellant samples were extruded, dried, and machined (refs 6 and 7) while the two non-polymer explosive samples were cast and machined to size (ref 4). Precautions were taken to insure that the cylinder end faces were adequately flat and parallel. The filler particle sizes are in the micron range for all composites. The densities of all samples were measured and results are presented only for samples having densities in a narrow range close to the maximum theoretical (zero porosity) density. In table 1, the composition of the explosive and propellant composites considered are given and in addition the glass transition temperatures, Tg, are given where known.

RESULTS

For uniaxial compression of the materials of the table, the stress initially increases linearly with increasing strain, then curves over the passes through a maximum stress with further increases in strain. The stress either decreases continuously for additional increases in strain beyond the maximum stress at higher temperatures or decreases abruptly to near zero at or just beyond the maximum stress at lower temperatures. Three quantities

Table 1
Composition of polymer composites and other materials

| | Name | Particulate | Binder | | TG(°C) |
			Polymer	Plastizer	
I	Pax 2	HMX - 80%	CAB - 8%	BDNPA/F - 12%	-37[a]
II	Pax	HMX - 85%	CAB - 6%	BDNPA/F - 9%	-37[a]
III	9404	HMX - 94%	NC - 2%	CEF - 3.84%	-34[b]
IV	9501	HMX - 95%	ESTANE - 2.5%	BDNPA/F - 2.5%	-41 (B)[c]
V	9502	TATB - 95%	KEL F 800 - 5%		30 (B)[b]
VI	LX-14	HMX - 95.5%	ESTANE 5702-F1 - 95.5%		-31 (B)[b]
VII	M30[d]	NQ - 48%	NC* - 28%	NG - 22%	-57[f]
VIII	M43[e]	RDX - 76%	CAB/NC - 12%/4%	BDNPA/F - 8%	
XIX	COMP B	RDX - 59.5%	TNT/WAX - 39.5%/1%		
X	TNT	TNT - 100%			

HMX - Cyclotetramethylene tetranitramine; TATB - 1,3,5-triamino-2,4,6-trinitrobenzene; RDX - Cyclotrimethylene trinitramine; NQ - Nitroguanadine; TNT - Trinitrotoluene; NC - Nitrocellulose; NG - Nitroglycerine; CAB - Cellulose acetate butyrate; BDNPA/F - Bis(2,2-dintropropyl)acetal/formal; CEF - Tris(beta chloroethyl) phosphate; ESTANE - Poly-urethane; KEL F 800 - Chlorotrifluoroethylene/vinylidine floride copolymer; B - Property of the binder

---

*Also contains 2% ethyl centralite.

[a]Personal communication, J. Harris, Picatinny Arsenal, NJ.

[b]Reference 8.

[c]Personal communication, G. L. Flowers, Mason & Hanger-Silas Mason Co, Inc, Pantex Plant, Amarillo, TX.

[d]Data taken from reference 6.

[e]Data taken from reference 7.

[f]References 9 and 10.

taken from the stress versus strain curves are of interest; the initial slope which is taken as a measure of the modulus (E), the maximum compressive stress [the compressive strength (σ_m)], and the strain at the maximum stress (ε_m).

Linear relationships between σ_m and E and a constant ε_m were found for all materials with changes in temperature and strain rate. However, the temperature (and strain rate) ranges for this linearity between σ_m and E, and constant ε_m vary with the material. For composites III, IV, V, and VII (group A), this linear range and constant ε_m covers approximately the whole measured temperature (and strain rate) range from -45° to 75°C, while for composites I, II, VI, and VIII (group B), the linear relationship and constant ε_m are only valid from approximately 0° to 65°C. The linear relationship is also observed for composite IX and TNT (X) from 20° to 60°C, the only temperature range for which data is available at this time. These results are illustrated in figures 1 and 2 for composite III. A more detailed report containing the results for all of the composites and other explosives will be published at a later date. σ_m and E change by at least an order of magnitude over the linear range of figure 1, while the data of figure 2 indicates that ε_m is approximately constant for these same conditions. The larger scatter in the data of figure 1 at low temperatures compared to the higher temperatures is associated with increased brittleness at the lower temperatures. The results for the other composites of group A are similar to those of figures 1 and 2. The results for the other materials are similar to those of figures 1 and 2 for the high temperature range (above 0°C), but for the composites of group B in the low temperature range (below 0°C) σ_m lies below an extrapolation of a straight line through the high temperature points of plots similar to that of figure 1. In addition, ε_m for group B is smaller in the low temperature range than in the high temperature range (fig. 2). Data is available for at least four strain rates for composites II, III, IV, V, and VI; several strains rate for composite I; two strain rates for composites IX and TNT; and one strain rate for composites I, VI, VII, and VIII.

From the stress versus strain curve, the relationship between three quantities σ_m, E, and ε_m can be shown to be

$$\sigma_m = E\,\varepsilon_m/(1 + a) \tag{1}$$

where $(1 + a)\,\sigma_m$ is the stress at which the straight line through the initial linear portion of the stress versus strain curve, the slope of which defines E, intersects a constant strain line at ε_m (ref 2). a is a measure of the shape of the stress versus strain curve between the point where it deviates from the initial straight line and the point of maximum stress. A linear relationship between σ_m and E and a constant ε_m then requires $(1 + a)$ to be constant to satisfy this equation. While the parameter a does change somewhat with temperature, the magnitudes and changes in a are such that equation 1 is satisfied by data of the type of figures 1 and 2 for all of the materials of the table within the precision of the measurements and within the temperature limits given previously.

At the lowest temperatures all polymer composites give evidence of abrupt fracture, i.e., an abrupt decrease of the stress with increasing strain at strains equal to or greater than the strain at the maximum stress. In addition--at the lowest temperatures--composites I, II, VII, and VIII fracture-fragment into many many pieces, while composites III, IV, V, and VI fracture into several pieces. At the highest temperatures, in contrast, all polymer composites deform extensively in a plastic like manor and do not show the abrupt decrease of stress with increasing strain. At the highest temperatures--composites I, II, VII, and VIII exhibit some cracking at large strains while composites III, IV, V, and VI tend to fracture at large strains. The transition from the low to high temperature behavior is gradual with increasing temperature and is somewhat strain rate dependent. Composite V, which has a significantly higher Tg than the others, shows the transition from the low to high temperature behavior at a higher temperature. Data is not available in the low temperature range for composite XIX and TNT, but at the higher temperatures these materials fracture into several pieces without giving evidence of extensive plastic deformation (ref 4).

For composites of group B, the high temperature range, as discussed here, corresponds approximately to the temperature range of constant ε_m and proportionally between σ_m and E. In contrast, the strain is constant over the whole temperature range measured for composites of group A. In addition, σ_m is proportional to E over most of the temperature range for this group of composites. Therefore, most of the group that fragment into many many pieces at low temperatures do not have a constant strain or σ_m proportional to E in the low temperature range, while most of the group that fracture but do not fragment do have a constant strain and σ_m proportional to E over most of the temperature range.

DISCUSSION

There are several possible approaches to interpreting these results. In one approach, the condition for failure is taken as a strain and ε_m a measure of this strain. Consider that failure initiates at the point where the stress versus strain curve deviates from linearity in the initial portion of the stress versus strain curve and that at this point the stress and strain are σ_f and ε_f. σ_m and ε_m are then taken as measures σ_f and ε_f. This corresponds to approximately a 1% offset condition for most of the materials. The critical condition for failure is therefore a strain and not a stress as is the more usual case. This critical strain (or displacement) for failure could be due, for example, to a critical strain (or displacement) for irreversibly detaching the filler from the binder (interface failure) in the composites, or to other irreversible separations which do not depend on temperature and strain rate. Because ε_f (and so ε_m) is constant, σ_f (and so σ_m) is proportional to E, and since E changes with temperature and strain rate as expected for a viscoelastic material, σ_m has the same temperature and strain rate dependencies. Another way of viewing this process is to consider that the critical condition for failure is the stress necessary to produce a critical strain (or displacement), and this stress varies with temperature and strain rate because the critical strain is constant and the modulus varies with these parameters.

In another approach to interpreting these results, the stress is taken as the condition for failure as is the more usual case. However, the failure process (e.g., yield) must be such that the failure stress σ_f (and so σ_m) is proportional to the modulus. Therefore, ε_f (and so ε_m) will be constant. An example of this is the yield of glassy polymers at very low temperatures where the tensile yield strength is predicted and found to be proportional to the modulus with a proportionality constant between approximately 0.019 and 0.13 (refs 11 and 12). In contrast, the results here are for polymer-particulate composites primarily above Tg in compression with proportionality constants between 0.009 and 0.05.

G. A. has also observed an insensitivity of the failure strain to strain rate for M30 propellant (table 1) and has used a nonlinear viscoelastic model with damage to describe these results (ref 13). By fitting the model to the constant strain rate stress versus time data at the two extremes of strain rate, he has shown that the model correctly predicts the stress versus time data at two intermediate strain rates. The model gives a constant ε_m and correctly predicts other features of the data including the observed dependence of σ_m on strain rate. The model also indicates that the damage function is constant at ε_m as strain rate changes. However, the model does not appear to fit the data very well in the initial increasing stress portion of the stress versus time and so strain curves, and so the observed moduli are not apparently predicted. Additional work is required to determine if the model gives a constant ε_m as temperature is varied, and to apply the model to the other materials of the table.

Additional work is also required to determine the failure mechanism and so to distinguish between these or other approaches to failure. The results for composite IX and TNT indicate that the type of results obtained here are also valid for crystalline non-polymer organic materials. Because the results are similar for composite IX and the binder for this composite, TNT, it is probable that they are not attributable to interfacial failure in this composite, but rather to failure in the binder. Failure in this composite and in this binder are discussed elsewhere (ref 4). Further discussion of the failure mechanisms in all of the materials of the table will be given at a later date in another report.

The immediate practical importance of this work lies in the immense simplification to modeling mechanical failure in these materials by being able to use a strain criterion (for failure) which is constant over a wide range of temperatures and strain rates rather than a stress criterion which changes significantly with these two variables. In addition, evidence for a strain criterion for failure should stimulate theoretical work and additional experimental work.
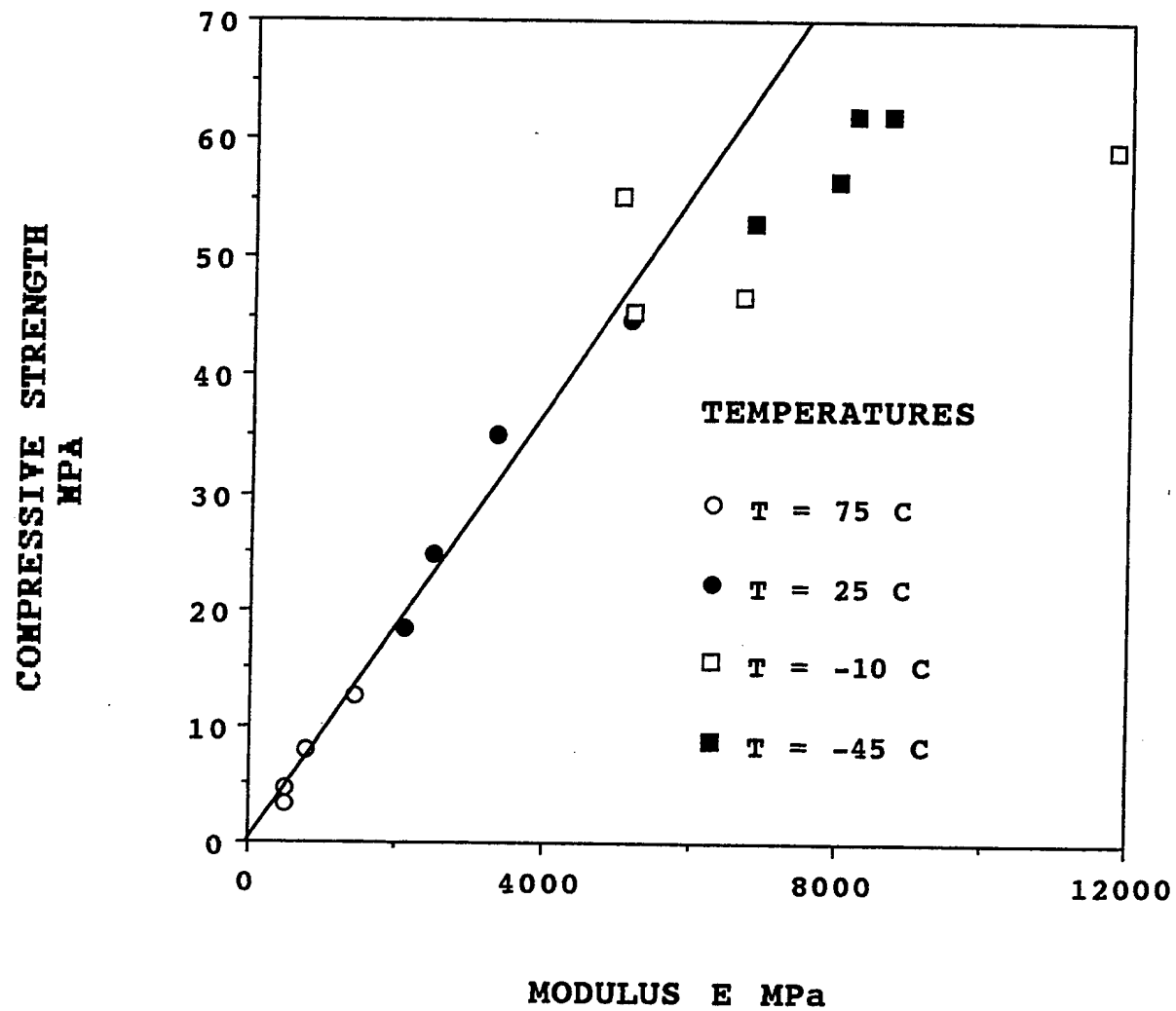
Data is given at each temperature for all four strain rates (fig. 2)

Figure 1
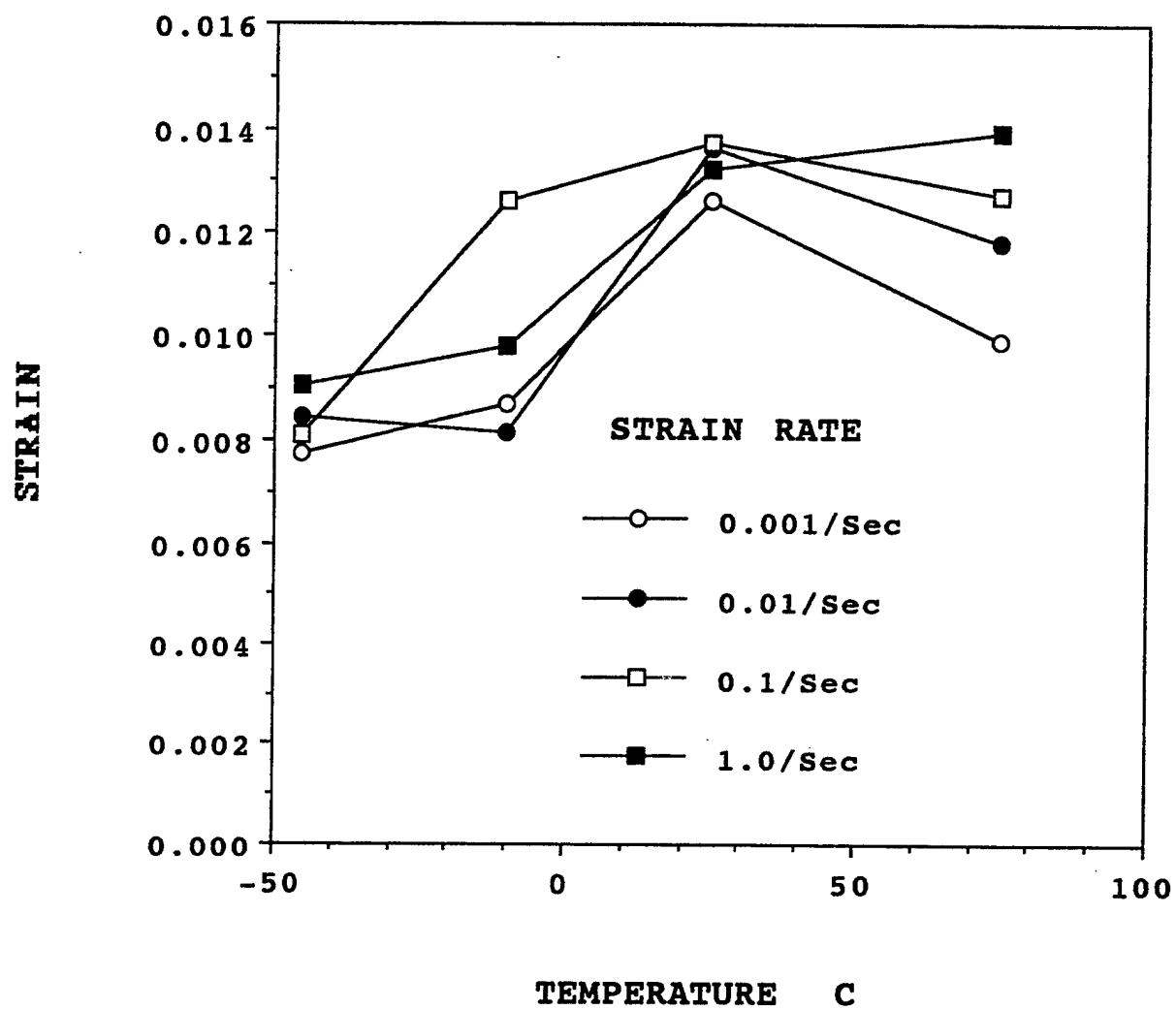Compressive stength (σ_m) versus modules (E) for composite III

Figure 2
Strain (ε_m) at the maximum compressive stress (compressive strength)
versus temperature for composite III

REFERENCES

1. Wiegand, D.; Hu, C.; Rupel, A.; and Pinto, J., "Fracture and Yield of Several Highly Filled Polymers," 9th International Conference on Deformation, Yield and Fracture of Polymers, The Institute of Materials, London, pp 64/1 - 64/4, 1994.

2. Wiegand, D., "Critical Strain for Failure of Highly Filled Polymer Composites," 3rd International Conference on Deformation and Fracture of Composites, University of Surrey Guildford, United Kingdom, pp 558 - 567, 1995.

3. Wiegand, D. A., "Constant Critical Strain for Mechanical Failure of Several Particulate Polymer Composites and Other Materials," Proceedings of the 20th Army Science Conference, In Press, 1996.

4. Wiegand, D.; Pinto, J.; and Nicolaides, S., "The Mechanical Response of TNT and a Composite, Composition B, of TNT and RDX to Compressive Stress: I Uniaxial Stress and Fracture," J. Energetic Materials, 9, pp. 19 - 80, 1991.

5. Wiegand, D., "Bond Strength of Pressed Composites," Materials Research Society Symposium Proceedings, Interface Control of Electrical, Chemical and Mechanical Properties, eds. Murarka, S.P.; Rose, K.; Ohmim, T.; and Seidel, T., Vol 318, pp. 387 - 392, 1994.

6. Lieb, R. J. and Leadore, M. G., "Correlation of the Failure Modulus to Fracture-Generated Surface Area in Uniaxially Compressed M30 Gun Propellant," ARL-TR-307, Army Research Laboratory, Aberdeen Proving Ground, MD, November 1993.

7. Lieb, R. J., "Correlation of the Failure Modulus to Fracture-Generated Surface Area in Uniaxially Compressed M43 Gun Propellant," ARL-TR-884, Army Research Laboratory, Aberdeen Proving Ground, MD, October 1995.

8. Dobratz, B. M. and Crawford, P. C., LLNL Explosives Handbook, Properties of Chemical Explosives and Explosive Simulants, Lawerence Livermore National Laboratory, Report UCRL-52997, Change 2, p. 6-6 and 6-8, 1985.

9. Nicolaides, S.; Pinto, J.; and Wiegand, D. A., Mechanical Properties, Mechanical Grain Failure and Changes in the Burning Performance of Gun Propellant, Chemical Propulsion Information Agency Publication 315, 1980.

10. Nicolaides, S; Wiegand, D. A.; and Pinto, J. J., "The Mechanical Behavior of Gun Propellant Grains in Interior Ballistics," Technical Report ARCLD-TR-82010, ARDC, Dover, NJ, 1982.

REFERENCES (cont)

11. Bowden, P. B. and Raha, S., "A Molecular Model for Yield and Flow in Amorphous Glassy Polymers Making Use of a Dislocation Analogue," Phil Mag 77, pp 150 - 166, 1974.

12. Argon, A. S. and Bessonov, M. I., Plastic Deformation in Polyimides with New Implications on the Theory of Plastic Deformation of Glassy Polymers, Phil Mag 35, pp 917 - 933, 1977.

13. Gazonas, G. A., "A Uniaxial Nonlinear Viscoelastic Constitutive Model with Damage for M30 Gun Propellant," Technical Report ARL-TR-115, Army Research Laboratory, Aberdeen Proving Ground, MD, 1993.

DISTRIBUTION LIST

Commander
Armament Research, Development and Engineering Center
U.S. Army Tank-automotive and Armaments Command
ATTN: AMSTA-AR-LSL (2)
           AMSTA-AR-GCL
           AMSTA-AR-AEE-W, N. Slagg
           AMSTA-AR-AEE-WW, B. Fishburn
                          M. Mezger
                          Y. Lanzerotti
                          D. Wiegand (15)
                          C. Hu
                          S. Nicolish
                          E. Baker
                          R. Surapaneni
           AMSTA-AR-AES
           AMSTA-AR-AEE, J. Lannon
           AMSTA-AR-AEE-B, D. Downs
                          S. B. Bernstein
           AMSTA-AR-QAR-R, L. Manole
                          E. Bixon
           AMSTA-AR-CCH-V, F. Hildebrant
           AMSTA-AR-AEE-BR
           AMSTA-AR-AET-M, R. Rupel
                          S. Cytron
Picatinny Arsenal, NJ 07806-5000

Commander
U.S. Army Production Base Moderniation Agency
ATTN: AMSMC-PBM, A. E. Siklosi
                      D. Fair
Picatinny Arsenal, NJ 07806-5000

Defense Technical Information Center (DTIC)
ATTN: Accessions Division (12)
8725 John J. Kingman Road, Ste 0944
Fort Belvoir, VA 22060-6218

Director
U.S. Army Materiel Systems Analysis Activity
ATTN: AMXSY-EI
392 Hopkins Road
Aberdeen Proving Ground, MD 21005-5071

Director
U.S. Army Materiel Systems Analysis Activity
ATTN: AMXSY-D
Aberdeen Proving Ground, MD 21005-5006

Commander
Chemical/Biological Defense Agency
U.S. Army Armament, Munitions and Chemical Command
ATTN: AMSCB-CII, Library
Aberdeen Proving Ground, MD 21010-5423

Director
U.S. Army Edgewood Research, Development and Engineering Center
ATTN: SCBRD-RTB (Aerodynamics Technology Team)
Aberdeen Proving Ground, MD 21010-5423

Director
U.S. Army Research Laboratory
ATTN: AMSRL-OP-CI-B, Technical Library
        AMXBR-BLT, R. Frey
        AMXBR-BLC, J. Starkenberg
                  P. Baker
        AMXBR-TBT, R. Lieb
                  J. Rochehio
Aberdeen Proving Ground, MD 21005-5066

Chief
Benet Weapons Laboratory, CCAC
Armament Research, Development and Engineering Center
U.S. Army Tank-automotive and Armaments Command
ATTN: AMSTA-AR-CCB-TL
        AMSTA-AR-LCB-RA, J. Vasilakis
Watervliet, NY 12189-5000

Director
U.S. Army TRADOC Analysis Command-WSMR
ATTN: ATRC-WSS-R
White Sands Missile Range, NM 88002

Comander
Naval Air Warfare Center Weapons Division
1 Administration Circle
ATTN: Code 473C1D, Carolyn Dettling (2)
China Lake, CA 93555-6001

GIDEP Operations Center
P.O. Box 8000
Corona, CA 91718-8000

Office of the Secretary of Defense
OUSDA(A)
Director, Live Fire Testing
Washington, DC 20301-3110

Director
U.S. Army Aviation Research and Technology Activity
Ames Research Center
Moffett Field, CA 94035-1099

Commander
U.S. Army Missile Command
ATTN: AMSMI-RD-CS-R (DOC)
Redstone Arsenal, AL 35898-5010

HQDA (SARD-TR)
Washington, DC 20310-0001

Commander
U.S. Army Materiel Command
ATTN: AMCDRA-ST
5001 Eisenhower Avenue
Alexandria, VA 22333-0001

Commander
U.S. Army Laboratory Command
ATTN: AMSLC-DL
Adelphi, MD 20783-1145

Commandant
U.S. Army Infantry School
ATTN: ATSH-CD-CS0-OR
Fort Benning, GA 31905-5660

Commander
U.S. Army Aviation Systems Command
ATTN: AMSAV-DACL
4300 Goodfellow Blvd
St. Louis, MO 63120-1798

Commander
U.S. Army Research Office
ATTN: Chemistry Division
P.O. Box 12211
Research Triangle Park, NC 27709-2211

Commander
Naval Surface Warfare Center
ATTN: R10C, L. Roslund
R10B, M. Stosz
R13, J. Short
R. Bernecker
J. Forbes
Silver Spring, MD 20902-5000

Commander
Naval Weapons Center
ATTN: L. Smith
        A. Amster
        R. Reed, Jr.
China Lake, CA 93555

Commander
Ballistic Missile Defense Advanced Technology Center
ATTN: D. Sayles
P.O. Box 1500
Huntsville, AL 35807

Air Force Armament Technology Laboratory
ATTN: AFATL/DOIL
        AFATL/DLODL
Eglin Air Force Base, FL 32542-5438

Southwest Research Institute
ATTN: M. Cowperthwaite
6220 Culebra Road
Postal Drawer 28510
San Antonio, TX 78284

New Mexico Institute of Mining and Technology
ATTN: TERA, T. Joyner
Campus Station
Socorro, NM 87801

Director
Lawrence Livermore National Laboratory
ATTN: R. McGuire
        K. Scribner
        M. S. Costantino
        L-324
        M. Finger
P.O. Box 808
Livermore, CA 94550

Director
Los Alamos National Laboratory
ATTN: J960, J. Ramsay
        MS B221, J. Dienes
        MS P952, J. Dick
        MS J567, D. J. Funk
P.O. Box 1663
Los Alamos, NM 87115

Southwest Research Institute
ATTN: H. J. Gryting
P.O. Box Drawer 28510
San Antonio, TX 78284

Honeywell, Inc.
ATTN: R. Tompkins
10400 Yellow Circle Drive
MN 38-330
Minnetonka, MN 55343

Commander
U.S. Army Armament, Munitions and Chemical Command
ATTN: AMSMC-ESM, W. D. Fortune
        AMSMC-IRD, G. H. Cowan
Rock Island, IL 61299-6000

Director
Sandia National Laboratory
ATTN: MS 432, J. Aidun
        MS 437, R. Thomas
        MS 477, T. Chen
Box 5800
Albuqure, NM

Johns Hopkins University
Applied Physics Laboratory
Chemical Propulsion Information Agency
ATTN: John Hannum
Johns Hopkins Road
Laurel, MD 20707

Morton Thiokol, Inc.
Louisiana Division
ATTN: Lee C. Estabrook
P.O. Box 30058
Shreveport, LA 71130

Commander
Naval Weapons Station
ATTN: L. Rothstein
        Code 50 - NEDED
Yorkstown, VA 23491